Materials and Design 58 (2014) 12–18

Contents lists available at ScienceDirect

Materials and Design

journal homepage: www.elsevier.com/locate/matdes

Effect of copper on the mechanical properties of alloys formed by powder metallurgy

Wilbert D. Wong-Ángel [a,*], Lucia Téllez-Jurado [a], José F. Chávez-Alcalá [a], Elizabeth Chavira-Martínez [b], Víctor F. Verduzco-Cedeño [c]

[a] Instituto Politécnico Nacional-ESIQIE, Depto. Ing. Metalurgia y Materiales, Zacatenco, A.P. 07738, México D.F., Mexico
[b] Universidad Nacional Autónoma de México, Instituto de Investigaciones en Materiales, A.P. 70-360, 04510, México D.F., Mexico
[c] Instituto Politécnico Nacional-ESIME, Edificio 5, 2do Piso, Zacatenco, A.P. 07738, México D.F., Mexico

ARTICLE INFO

Article history:
Received 25 September 2013
Accepted 2 February 2014
Available online 5 February 2014

Keywords:
Powder metallurgy
Copper addition
Density
Stress analysis

ABSTRACT

Alloys formed by powder metallurgy are typically porous, which reduces their strength. In this study, we attempt to improve the mechanical properties of an alloy composed of 0.6 wt% C, 1.0 wt% Ni, 0.3 wt% Mo, 0.7 wt% Mn and the balance Fe by addition of 8 wt% Cu. To form the alloys, powders are blended and compacted in a dual-action hydraulic press and then sintered in a furnace at 1150 °C. Alloys with and without Cu are used in specific parts designed for impact testing. Stress analysis is performed using ANSYS, which validates the operation of the parts. The strength of the body geometry according to its design is determined by considering the manufactured material and the loads that it is subjected to during operation. SEM images revealed that the alloy without Cu contains martensite and bainite phases with large, irregular pores. In contrast, the alloy with Cu has a considerably lower pore concentration. During sintering, Cu forms a liquid phase that can fill the spaces between the particles of the alloying powders. The result is an alloy with increased density and toughness; the density of the alloy increases from 7.2 to 7.8 g/cm^3 upon addition of Cu, and its toughness increases from 22 to 34 J.

© 2014 Elsevier Ltd. All rights reserved.

1. Introduction

With the growing demand for metallic components in the metalworking industry, powder metallurgy (PM) can be used to produce components with complex geometries, reduce machining costs and compete with other forming processes for large-scale production [1]. PM can be used to form multiple compositions by blending pre-alloyed or elemental powders [2]. However, the elements obtained using PM are porous. Generally, components that are subjected to impact loads during their operation are manufactured from steels produced by a continuous caster. Components produced by PM with the ability to tolerate high stresses can be obtained by sinter hardening, which yields a microstructure such as tempered martensite or bainite.

To produce good-quality components using PM, the porosity distribution must be homogeneous because heterogeneity has a negative effect on mechanical properties [3,4]. The porosity of components produced by PM is usually in the range of 5–15% depending on the compressibility of the alloying powders, carbon content and added lubricant. The pores are potential crack initiation sites, and can also guide and propagate cracks through the material. According to Bergmark and Alzati [5], a strong microstructure may be obtained by incorporating small amounts of alloying elements to compensate for the microcracks formed by pores.

Copper (Cu) is the most common alloying element added in powder form because of its low cost, availability and ability to improve the properties of alloys. Cu powder is blended with the master alloy, alloying element(s), lubricant and graphite. Cu can have a large effect on the mechanical performance of the resulting material. Copper melts at 1083 °C [6] and disperses well in the master alloy because of the capillary forces present as a result of the transition to a liquid phase during the sintering process. As a result, Cu helps to increase the toughness and density of the resulting alloys by filling pores [7]. The ability of Cu to improve the properties of alloys has been demonstrated. For example, Sanderow and Rivest [8] found that Cu infiltration provided a mix of phases that improved the mechanical properties and tempered hardness of prealloyed steel powders. Chawla et al. [9] determined that addition of 1.5 wt% Cu to an alloy containing Fe, Mo and graphite resulted in an increase in proportional limit stress, ultimate tensile

* Corresponding author. Tel.: +52 55 5729600x54209; fax: +52 55270.
E-mail address: wwonga0900@alumno.ipn.mx (W.D. Wong-Ángel).

http://dx.doi.org/10.1016/j.matdes.2014.02.002
0261-3069/© 2014 Elsevier Ltd. All rights reserved.

Table 1
Chemical compositions and properties of alloys.

	Fe (%)	C (%)	Ni (%)	Mo (%)	Mn (%)	Cu (%)	Apparent density (g/cm^3)	Flow rate (s/100 g)
Alloy 1 (without Cu)	97.42	0.6	1	0.86[a]	0.12[a]	–	3.13	58.2
Alloy 2 (with Cu)	89.42	0.6	1	0.86[a]	0.12[a]	8	3.5	56.8
Particle size (μm)	<10	45	40	25	45	33		

[a] Prealloyed.

Table 2
Mechanical properties of the alloys following sinter hardening.

Material	Elastic limit (MPa)	Tensile strength (MPa)	Young's modulus	Poisson's ratio	Hardness (HRc)	Toughness (J)	Density (g/cm^3)
Alloy 1 (without Cu)	520	1600	160	0.28	30	22	7.2
Alloy 2 (with Cu)	480	690	155	0.28	35	34	7.8

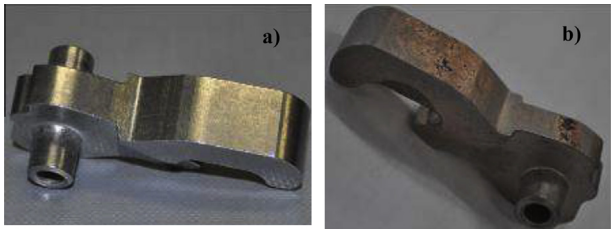

Fig. 1. Photographs of parts composed of (a) Alloy 1 without Cu and (b) Alloy 2 with Cu.

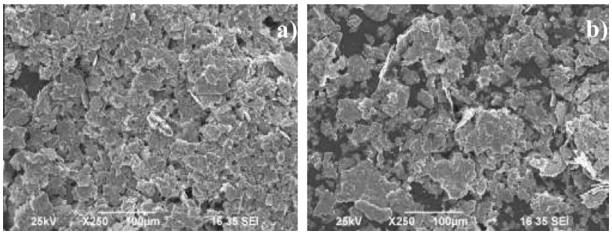

Fig. 3. SEM micrographs of the alloys after 10 h: (a) Alloy 1 without Cu and (b) Alloy 2 with Cu.

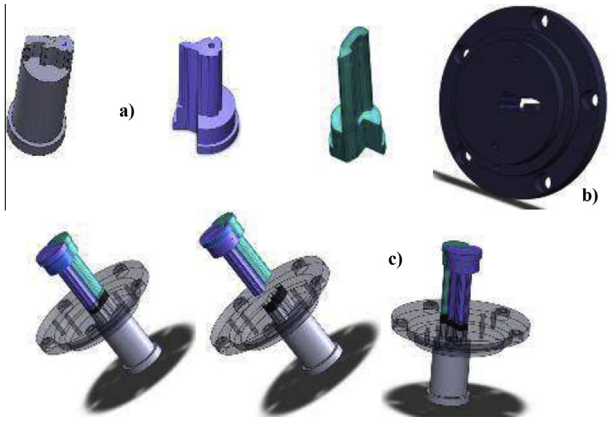

Fig. 2. (a) Compaction punches, (b) compaction matrix, and (c) the compaction tool ensemble used to produce parts.

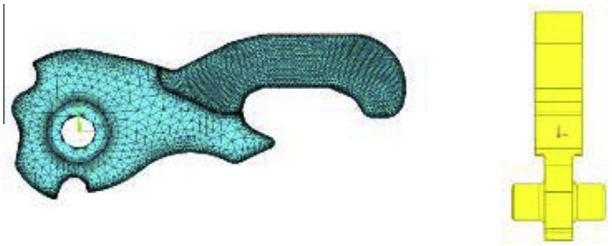

Fig. 4. Center of mass of the analyzed part.

strength, and fatigue strength over those of the Cu-free alloy. Takaki et al. [10] investigated the tensile properties and grain size of alloys containing 0–4 wt% Cu. They found that an increased proportion of martensite, which increased with Cu content, improved the strength-ductility balance of the alloys. Lowhaphandu and Lewandowski [11] examined the effect of infiltration of 10 vol% Cu on the monotonic fracture resistance and fracture crack growth behavior of PM-processed porous plan carbon steels exposed to different heat treatment conditions. They found that the Cu-infiltration samples possessed superior fracture toughness and fatigue properties compared with the porous matrix material lacking Cu. Bernier et al. [12] helped to improve our understanding of the role of Cu in strengthening sintered steel parts through detailed characterization of the microstructure, hardness and transverse rupture strength of Cu-infiltrated steel samples. They quantified the strengthening effect of Cu in pearlite and martensite and observed nanometer-sized copper precipitates in the doped steel

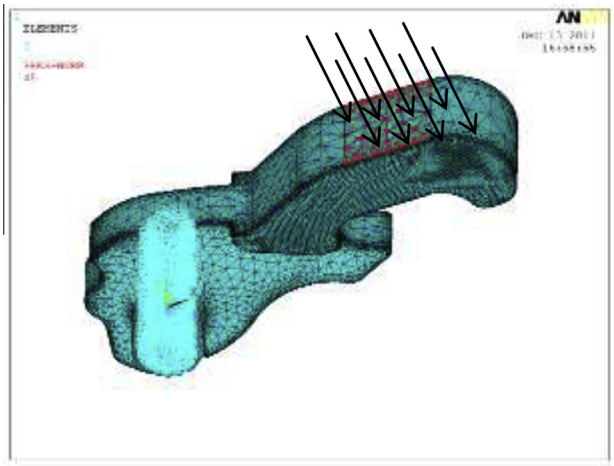

Fig. 5. Direction and placement of impact on part.

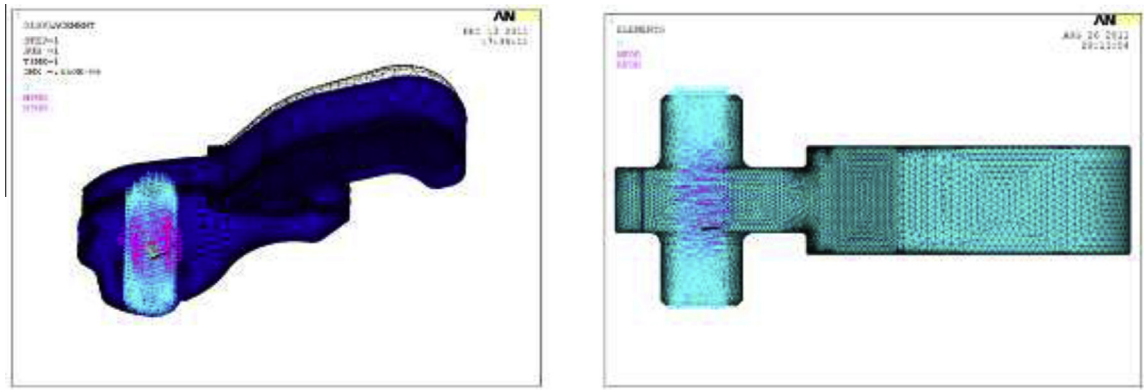

Fig. 6. Displacement restrictions for stress analysis.

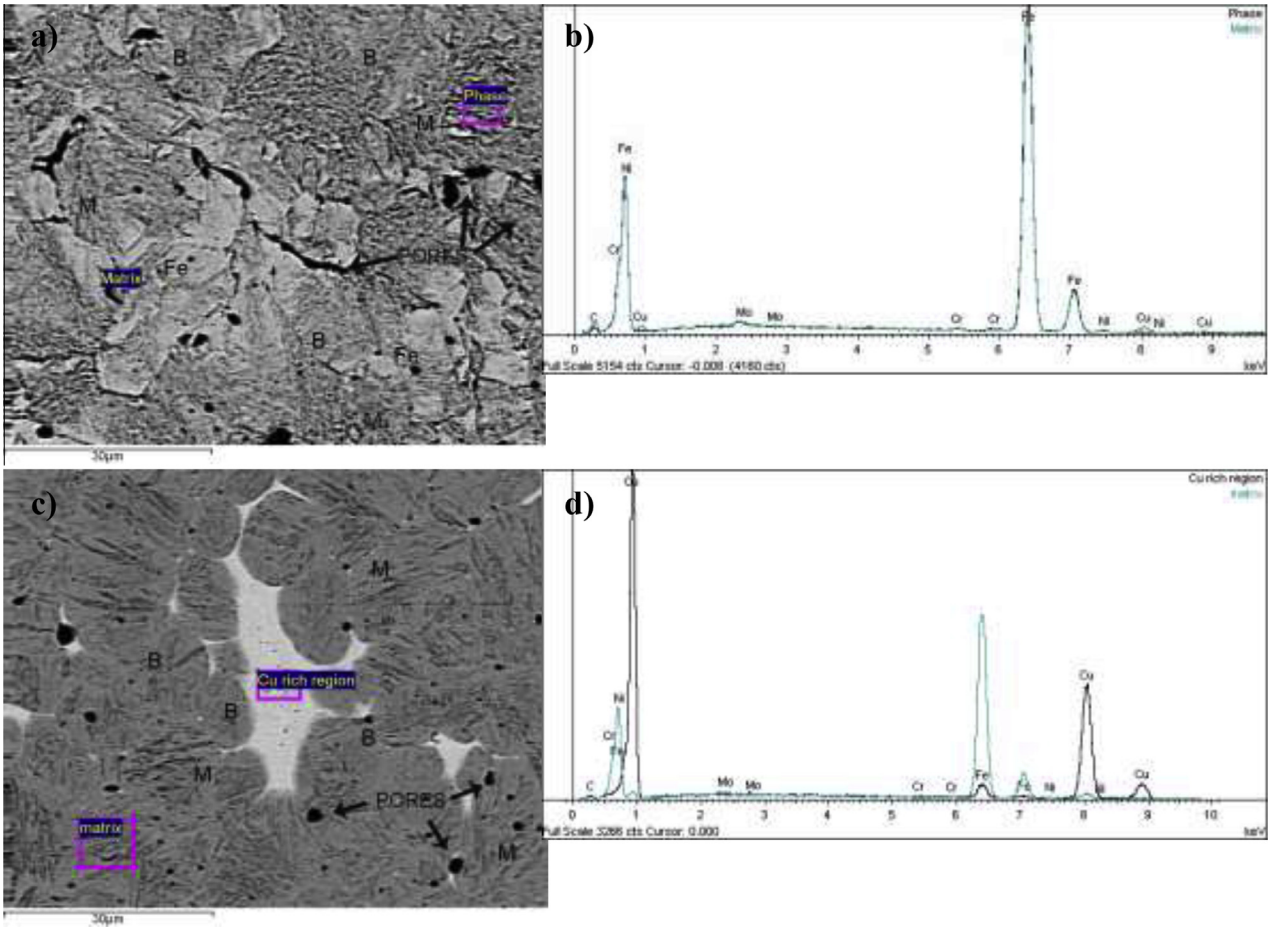

Fig. 7. (a) SEM image and (b) corresponding EDS of the indicated regions in Alloy 1. (c) SEM image and (d) corresponding EDS of the indicated regions in Alloy 2. M = martensite, F = ferrite, B = bainite.

samples. Inclusion of Cu can improve the mechanical properties of alloys because it promotes the formation of secondary pores that are much smaller than the larger primary pores associated with the sintering of ferrous alloys lacking Cu [9].

In this study, the effect of Cu addition to the alloy containing 0.6% C, 1.0% Ni, 0.3% Mo, and 0.7% Mn and the balance Fe is examined. Cu powder is mixed with the alloy and then sintered. Alloys with and without Cu are shaped into a complex part: the firing hammer of a gun, which is subjected to high impact during operation. It was anticipated that Cu would improve the ductility of the firing hammer. The effect of Cu on the fracture behavior, microstructure and porosity of the part is examined. The stresses and strains that the component manufactured using PM are subject to during operation are determined both experimentally and by finite element analysis (FEA).

2. Experimental details

2.1. Part design

The wrought components subjected to impacts under the same conditions were manufactured by cold forging at a pressure of 400

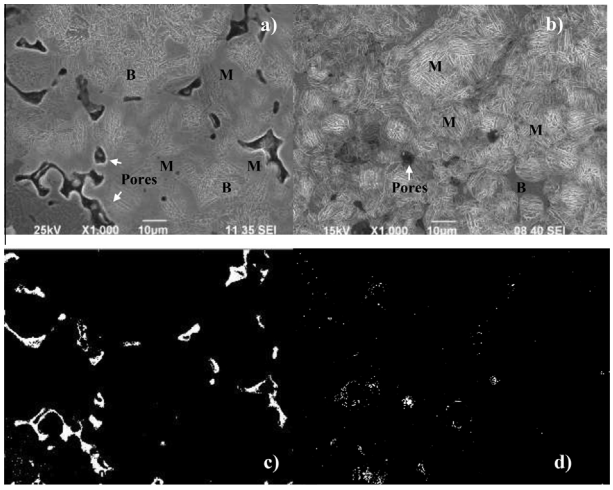

Fig. 8. SEM images of (a) Alloy 1 without Cu, (b) Alloy 2 with Cu, and the pores in (c) Alloy 1 and (d) Alloy 2.

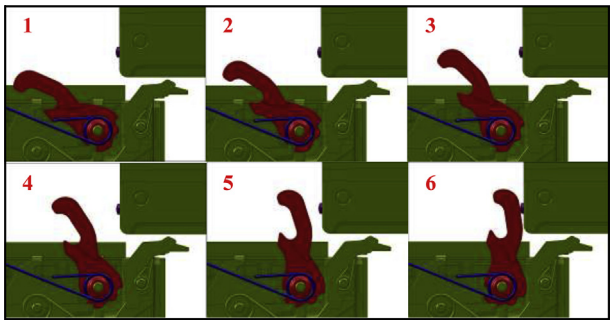

Fig. 9. Process of the operational test of parts composed of Alloys 1 and 2.

MPa. After machining, thermal treatment was required to improve the mechanical properties of the alloys. As a result, the manufacturing process requires a long time to produce the final part. Fig. 1 shows photographs of the part subjected to impact.

CAD (SolidWorks 2010) was used for geometric modeling of the part subjected to impact and the powder compacting toolkits. The toolkits (Fig. 2) were manufactured using a vertical machining center (VCN 510-II, Mazak, Nexus, Florence, Kentucky) with tool grade steels AISI D2 for the matrix and AISI O1 for the compaction punches.

2.2. Materials

Pre-alloyed powders (Ancorsteel 85 HP, containing Mn 0.12 wt%, Mo 0.86 wt%, C 0.01 wt% and the balance Fe) with particle sizes less than 50 μm along with 1 wt% Ni and 0.6 wt% C were used to form Alloy 1 containing 0.6 wt% C-1.0 wt% Ni-0.3 wt% Mo-0.7 wt% Mn and the balance Fe, and Alloy 2 containing the components of Alloy 1 and 8 wt% Cu was also fabricated. The properties of the pre-alloyed powders are shown in Table 1.

The powders were mixed in a custom-made horizontal mill that was 15.2 cm long and 12.5 cm in diameter with a ball load of 2461 g and ball/powder weight ratio of 36:1 for 10 h under an argon atmosphere to avoid oxidation of the alloying element (Cu). Zinc stearate 0.8 wt% was added as a process control agent. Scanning electron microscopy (SEM, JEOL, JSM 6490, Peabody, Massachusetts, USA) was used to observe the morphology of the alloys produced at the back of the mill, as shown in Fig. 3a and b. Milling

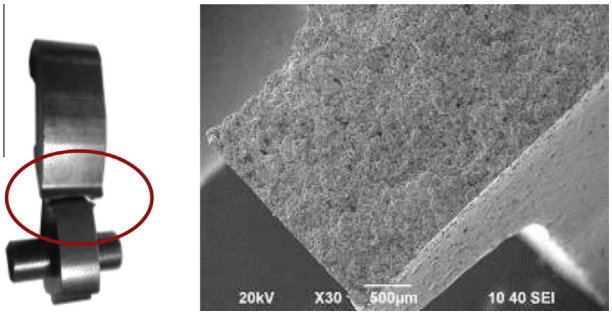

Fig. 10. Fracture of the part composed of Alloy 2 after operational testing.

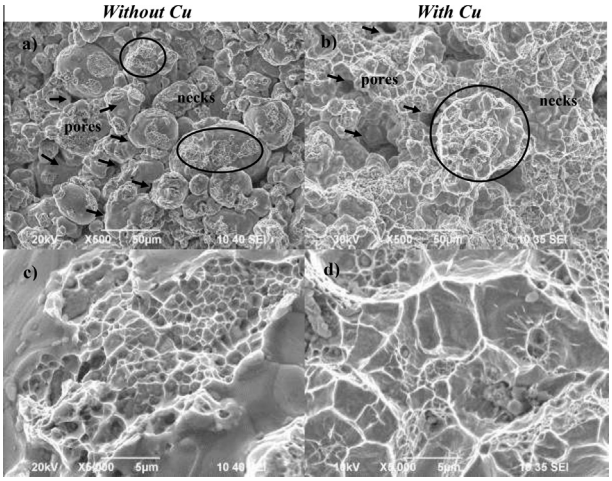

Fig. 11. SEM images of the fracture surfaces of parts composed of (a), (c) Alloy 1, and (b), (d) Alloy 2.

caused the particle size to decrease to 10–50 μm and flakes to form, which should help the compaction process [13].

2.3. Compaction and sintering

The alloys with and without Cu were compacted using a dual-action hydraulic press (RPS 400, Lauffer, GmbH & Co., Germany) with a 400-ton capacity at a speed of 40 mm s^{-1} using the tools fabricated for part forming (Fig. 2). The green density of the pellets was measured using a bushing-type exterior micrometer (0–25 mm, resolution: 0.001 mm, Model 293, Mitutoyo America Co., Aurora, USA). The compacted materials were sintered in a furnace (Mahler GmbH, Germany) under an argon atmosphere by pre-sintering at 500 °C for 30 min, sintering at 1150 °C for 40 min, and then sinter hardening in the rapid cooling area at a cooling velocity of 1 °C s^{-1} [14]. The density of the sintered alloys with and without Cu was determined by the gravimetric immersion method described in Metal Powder Industries Federation standard 35 [15].

For the sample containing Cu, a tensile test was performed using a universal indenter (AG 250 kN IC, Shimadzu, Japan) with a 25-ton capacity according to ASTM: E-8/E8M-13a. Impact tests were performed using a pendulum Charpy tester (JBW-300 PTE, Shandong, China) according to ASTM: E-23-12c. The mechanical properties of the alloys are summarized in Table 2.

2.4. Finite element analysis

A model of the parts was created using the CAD software Solid Works Version 2011 as the design platform. FEA was performed using ANSYS 12.0 by selecting a solid structural element of 8 nodes

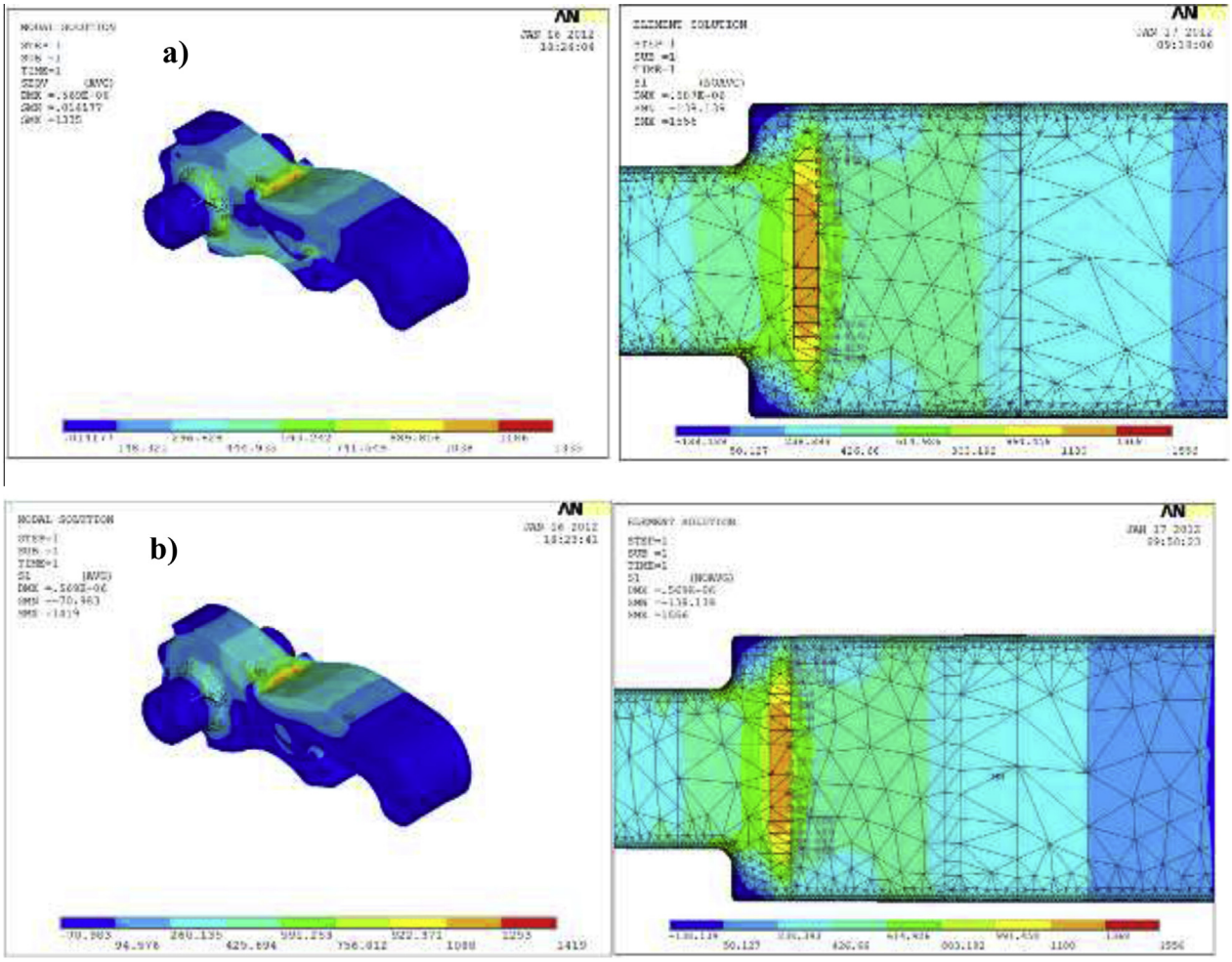

Fig. 12. Calculated stress levels for parts composed of (a) Alloy 1 without Cu and (b) Alloy 2 with Cu.

for the 3D simulations (Solid187) [16]. The impact loads of these parts were derived from the actuation of shocks or springs that provide, on average, between 30 and 50 N. These can be single-acting, repetitive, semiautomatic, or automatic. These forces were applied at a determined distance from the pivot point, which is the center of mass of the part. In this case, the distance was 13.00 mm along the *X*-axis and 3.61 mm along the *Y*-axis from the pivot point toward the impact zone of the part; this distance is on the midline plane of the part, as shown in Fig. 4. The average force generated by the actuation of the part was 45 ± 5 N. The impact force was applied uniformly to the flat area on the top of the part, as shown in Fig. 5. Meshing of the part was performed in the ANSYS platform considering the mechanical properties of the alloys (Table 2; i.e., Young's modulus of 1.6×10^{11} and 1.55×10^{11} for alloys 1 and 2, respectively, and a Poisson's ratio of 0.28). Finally, the model was discretized into 414,569 elements and 82,223 nodes. In the pre-process stage, the impact consisted of a force of 45 ± 5 N applied uniformly over the top flat area of the part (Fig. 5), restricting the virtual model in the zone of the pivot axis as shown in Fig. 6.

3. Results and discussion

3.1. The effect of Cu on alloy microstructure

SEM images and corresponding EDS of the alloys were consistent with the presence of martensite and bainite in a ferritic matrix (Fig. 7a and b). Fig. 8a and b shows that Alloy 2 containing Cu possessed a larger area fraction of martensite than Alloy 1. Alloy 1 contains aligned, interconnected pores, and small necks between the particles (Fig. 8c). The coalescence of pores is the origin of localized brittle fracture, which decreases the macroscopic ductility of materials obtained using PM [17]. Fig. 8d shows the isolated pores in Alloy 2, which provide increased macroscopic ductility compared with that of Alloy 1. The total porosity, and size, shape, and separation of pores are important factors affecting fatigue and impact behavior in materials obtained using PM [18]. Our observations are consistent with the findings of Gonobadi [19], who reported that increasing austenitizing temperature during heat treatment increases the amount of Cu dissolved in austenite, which increased the volume percent of martensite, as well as the hardness and strength of the final material.

3.2. Operational tests of the parts

The parts formed of each alloy were subjected to an operational test where a rotation point was fixed in the lower area of the part and a force of 45 N was applied as developed in a spring, as shown in the series of images in Fig. 9. The parts were subjected to 15,000 operations at a rate of 40 operations per minute. During the operational test, the parts manufactured without Cu (Alloy 1) showed crack initiation and propagation at the regions of highest stress, spanning the transverse section of the part until brittle fracture occurs. The part fabricated using Alloy 2 with Cu tolerated 65% more

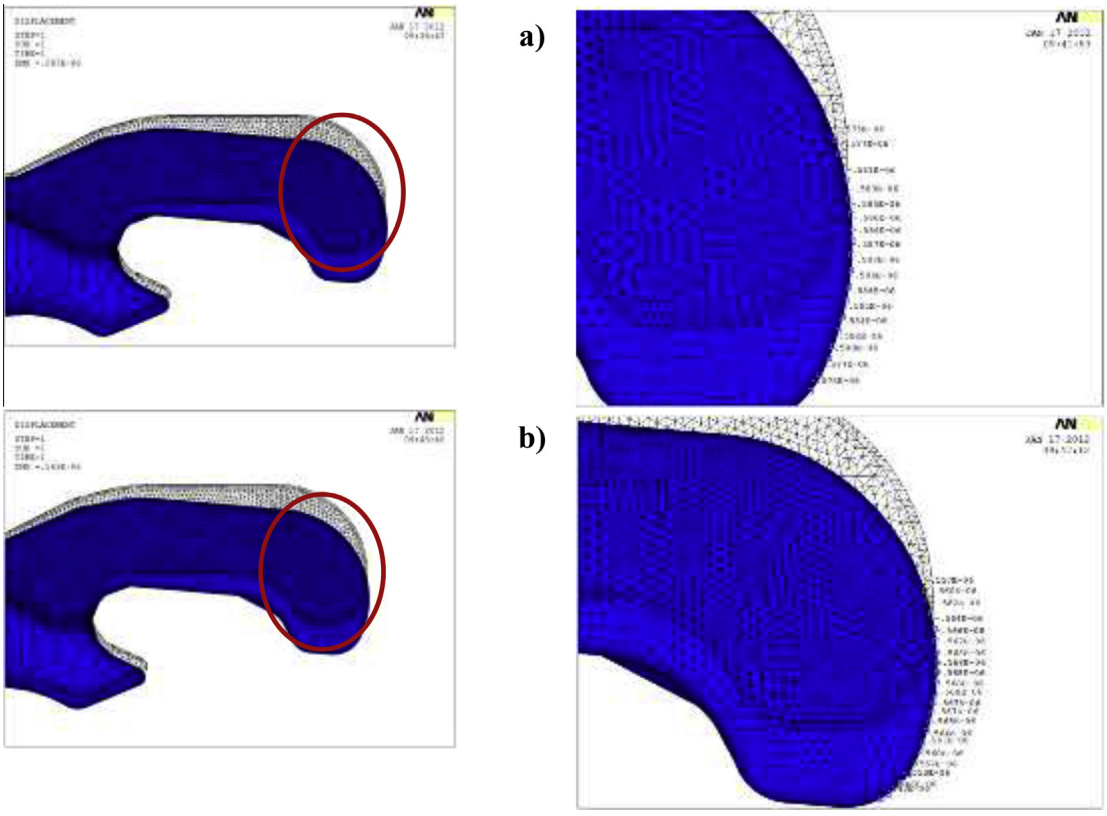

Fig. 13. Node displacement of the parts composed of (a) Alloy 1 without Cu and (b) Alloy 2 with Cu.

test cycles than that composed of Alloy 1 before failure by fracture, as shown in Fig. 10.

The fracture surface of both parts was observed by SEM, as shown in Fig. 11. The part without Cu shows brittle fracture, characterized by the presence of microcavities. The necks between particles break, and pores, which promote the formation of cracks and fracture, are also observed (Fig. 11a and c). The part composed of Alloy 2 has a higher density than that formed from Alloy 1, which increases neck size, and reduces the number the pores (Fig. 11b and d). The pore volume of each alloy determines its load-bearing ability. The stress concentration effect tends to be greater in samples with many large, irregular pores, so it is likely that the failure caused by fracture is initiated by the nucleation of cracks that start at these defects and propagate simultaneously until they coalesce into a larger crack. These observations are consistent with those of Carabajar et al. [20] and Lowhaphandu and Lewandowski [11], who found that the monotonic fracture properties of porous matrices and Cu-infiltrated composites vary considerably, as do their fatigue properties. These materials showed improved fracture properties upon Cu infiltration, but they still do not approach the level of wrought steels.

3.3. FEA of the parts

The parts composed of different alloys were modeled by FEA using the constitutive equations that govern material behavior. This system of equations is outlined by Hooke's Law:

$$f = k\ u, \tag{1}$$

where f is force, vector u is the node displacements that are generated by the forces applied to the nodes and the k is rigidity of the component to be analyzed.

Stresses along the transverse section of each part were imposed on the top area (Fig. 12a and b) because this zone is considered critical for operation. The behavior of the material where it shows potential to fail was determined from node to node. The behavior of each part was then verified using the Tresca criterion ($\tau_{max} \geq \sigma y/2$). Minimal difference was observed between the parts composed of different alloys using the primary stress criterion along the critical zone of each part subjected to impact.

Fig. 13 shows the calculated displacement experienced by the nodes of the parts composed of different alloys after impact. Alloy 2 with Cu can tolerate greater elastic stress than Alloy 1 without Cu. This is because Cu increases the toughness and density of the alloy, which will lead to the possibility of higher elastic stresses. Higher density and toughness are achieved in the presence of Cu because it promotes liquid phase sintering, and can fill pores in the alloy.

4. Conclusions

The addition of copper to iron-based alloys formed by PM thickens the necks between particles and reduces porosity. This in turn increases the density and toughness of the Cu-doped alloy compared with that lacking Cu. As a result, complex parts formed from the alloys with and without Cu showed different mechanical properties and fracture behavior; the part composed of alloy containing Cu tolerated 65% more test cycles than that of the part lacking Cu. FEA allowed the source of failure during operation of the designed part to be determined as well as the zone experiencing the largest stresses.

Acknowledgements

The authors gratefully acknowledge the support from the Institute Polytechnic National and University Autonomous of Mexico (E.S.I.Q.I.E. and I.I.M). We also thank the General Directorate of

the Military Industry for providing elemental powder metallurgy samples and equipment.

References

[1] German RM. Powder metallurgy and particulate processing. Metal Powder Industries Federation; 2000.
[2] Zhang DL. Processing of advanced materials using high-energy mechanical milling. Prog Master Sci 2004;49:537–60.
[3] Sharma D, Chandra K, Misra PS. Design and development of powder processed Fe–P based alloys. Mater Des 2011;32:3198–204.
[4] Warke VS, Sisson Jr RD, Makhlouf RD. The effect of porosity on the austenite to ferrite transformation in powder metallurgy steels. Mater Sci Eng A 2011;528:3533–8.
[5] Bergmark A, Alzati L. Fatigue crack path in Cu–Ni–Mo alloyed PM steel. Fatigue Fract Eng Mater Struct 2005;28:229–35.
[6] Marucci ML, Hanejko FG. Effect of copper alloy addition method on the dimensional response of sintered Fe-Cu-C steels. Advances in Powder Metallurgy and Particulate Materials, MPIF 2010:1–11.
[7] Dong Y, Jun L, Wen J, Jie S, Kunyu Z. Effect of Cu addition on microstructure and mechanical properties of 15%Cr super martensitic stainless steel. Mater Des 2012;41:16–22.
[8] Sanderow H, Rivest P. Mechanical properties of copper-infiltrated low-alloy steels using wrought wire infiltant, in 'Advances in powder metallurgy & particulate materials', Part 2, 10. Princeton, NJ: MPIF; 2007.
[9] Chawla N, Babic D, Williams JJ, Polasik SJ. Effect of copper and nickel alloying additions on the tensile and fatigue behavior of sintered steels, in 'Advances in powder metallurgy & particulate materials', Part 5, 104. Princeton, NJ: MPIF; 2002.
[10] Takaki S, Fujioka M, Aihara S, Nagataki Y, Yamashita Y, Sano N. et al. Effect of Copper on Tensile Properties and Grain-Refinement of Steel and its Relation to Precipitation Behavior. Mater Trans 2005;45:2239–44.
[11] Lowhaphandu P, Lewandowski JL. Fatigue and fracture of porous steels and Cu-infiltrated porous steels. Metall Mater Trans A 1999;30A:325–34.
[12] Bernier F, Gauthier M, Plamondon P, L'Espérance G. Copper strengthening of PM steel parts. Int J Powder Metall 2011;47:11–9.
[13] Arik H, Turker M. Production and characterization of in situ Fe–Fe3C composite produced by mechanical alloying. Mater Des 2007;28:140–6.
[14] Hatami S, Malakizadi A, Nyborg L, Wallin D. Critical aspects of sinter-hardening of prealloyed Cr–Mo steel. J Mater Process Tech 2010;210:1180–9.
[15] Metal Powder Industries Federation MPIF Standard 35. Materials Standards for PM Structural Parts. 2012.
[16] ANSYS Release 11.0 (2009). Documentation for ANSYS, Elements Reference. 2002, Part I.
[17] Lindstedt U, Karlsson B, Masini R. Influence of porosity on the deformation and fatigue behavior of P/M austenitic stainless steel. Int J Powder Metall 1997;33:49–61.
[18] Christian KD, German RM. Relation between pore structure and fatigue behavior in sintered iron-copper-carbon. Int J Powder Metall 1995;31:51–61.
[19] Gonobadi HI. Physical and mechanical characteristics of heat treated PM parts, infiltrated by copper. Life Sci J 2013;10:86–91.
[20] Carabajar S, Verdu C, Fougères R. Damage mechanisms of a nickel alloyed sintered steel during tensile test. Mater Sci Eng A 1997;232:80–7.